River Flow 2012 – Murillo (Ed.)

Steep flume experiments with large immobile boulders and wide grain size distribution as encountered in alpine torrents

T. Ghilardi & A.J. Schleiss
Laboratory of Hydraulic Constructions (LCH), Ecole Polytechnique Fédérale de Lausanne (EPFL), Switzerland

ABSTRACT: Flow conditions and sediment transport capacity in steep mountain rivers are poorly known. One of the main problems is that the presence of macro-roughness elements, such as large relatively immobile boulders, have a strong influence. Experiments carried out in a steep laboratory flume, show that the bed surface occupied by boulders and their protrusion need to be taken into account for the estimation of sediment transport. The tests were performed with a wide mobile grain size distribution and a random position of the large boulders. A clear relationship between the dimensionless distance of boulders and sediment transport capacity is found. The bedload rate can be reduced by 60% when 15% of the bed surface is occupied by boulders, compared to transport rate without boulders. The boulder diameter also has an influence on sediment transport capacity. This is linked to both the surface occupied by the boulders and its average protrusion.

1 INTRODUCTION

Flow conditions and sediment transport are well known for lowland rivers. On the contrary, only few studies have been made on steep mountain channels, mainly during the last two decades. Most sediment transport equations, even if developed for high slopes, overpredict sediment flux by several orders of magnitudes in mountain streams. The reason is that sediment transport equations often don't take into account the flow resistance induced by the relatively immobile large boulders, which can occupy a large area of the riverbed.

Alpine rivers are typically characterized as streams having longitudinal slopes ranging from 0.1% to almost 20% or more (Papanicolaou et al., 2004). These gravel or boulder bed streams constitute an important part of the total channel length in mountainous regions. Most sediment reaching floodplains are mobilized on hillslopes and transit trough high-gradient torrents (Yager et al., 2007).

Gravel bed and boulder bed streams are characterized by a wide grain-size distribution that is composed of finer, more mobile sediment and large, relatively immobile grains or boulders (Rickenmann, 2001; Papanicolaou et al., 2004; Yager et al., 2007). It has been shown that in coarse gravel bed torrents the grain size distribution of the transported bedload approaches that of the bed material only for high flow intensities (Lenzi et al., 1999; Rickenmann, 2001). Ferro (1999) points out that many Sicilian and Calabrian gravel-bed streams have a bimodal bed particle size distribution, characterized by a fine and a coarse component. Moreover, in theses torrents, the water depth is small compared to the roughness elements. Large relatively immobile boulders can thus be considered as macro-roughness elements.

Most sediment transport equations estimate bedload transport rates based on the difference between critical and total shear stress. Macro-roughness elements induce a certain stress and disrupt the flow by altering the channel roughness (Yager et al., 2007). As Lenzi et al. (2006) underline, if the roughness increases due to the number of boulders, the form drag will also increase. This implies lower shear stresses available at the bed for sediment entrainment.

As proposed by many authors, a shear stress partitioning method is needed to take into account the presence of macro-roughness elements. Different parameters are proposed according to the authors for shear stress and bed resistance equations, but they generally resume to the number of boulders, their cross section, the bed area occupied by them, the distance between boulders and the drag coefficient (Bathurst, 1978; Canovaro et al., 2007; Yager et al., 2007). It is suggested (Yager et al., 2007), that only the part of the shear stress not acting on boulders will induce a sediment transport. Moreover, there is a limited sediment supply because of the bed area occupied by boulders. When commonly used sediment transport formula are adapted in order to take into account only the shear stress acting on mobile sediments and the limited sediment availability, the bedload estimation is deeply improved (Ghilardi et al., 2011; Yager et al., 2007). It has been shown that the presence of boulders decreases the sediment transport capacity (Ghilardi et al., 2011; Yager et al., 2007). Boulder dimensionless distance λ/D [−], where λ [m] is the average distance between boulders of diameter D [m], and protrusion P_{av} [m] are good proxies for sediment transport in mountain

streams. The influence of boulder diameter has not yet been studied. The present study will increase the knowledge on this matter.

The presence of a wide grain size distribution (GSD) in mountain rivers has a noticeable impact on bedload. Sediment transport rate fluctuations have been identified for the first time in the 1930 during field measurements. Lately, many authors started studying this phenomenon in experimental flumes (Recking, 2006; Bacchi et al., 2009; Iseya et al., 1987; Frey et al., 2003). Iseya et al. (1987) showed that a longitudinal sediment sorting occurs when a wide GSD is constantly fed into a flume. This segregation produces rhythmic fluctuation in the sediment transport rate. It is also pointed out that sediment particles availability, induced by a longitudinal sediment sorting, determine the magnitude of bedload transport rate and its fluctuation. According to the authors, two main factors cause sediment transport to fluctuate. Namely migrations of bedforms and segregation of the surface grain size distribution, with the formation of an armor layer.

Frey et al. (2003) showed by means of image analysis that some cyclic patterns are generally found in outgoing sediment discharge on steep flumes with a wide grain size distribution. The minimum outgoing discharge could be half of the maximum discharge. The outgoing sediment discharge and its grain size distribution were not independent. High solid discharges occurred for fine GSD outlet, whereas the GSD was coarser during the low sediment discharge event. This behavior was not encountered with a uniform grain size distribution. During the experiments, Frey et al. (2003) visually observed that a bed-armoring process was associated with transient antidune-like structures. These bedforms were increasing bed resistance and thus decreasing solid discharge. The armoring layer was then destroyed, leaving a finer bed in place with practically no bedforms. The highest outgoing sediments discharges were observed at this moment. The cyclic change in bedforms and thus GSD starts once again with the formation of an armoring layer.

2 EXPERIMENTAL FACILITY AND METHODS

In order to analyze the impact of randomly distributed boulders on sediment transport capacity, a series of experiments has been carried out. The tilting flume used for the research is 8 [m] long and 0.5 [m] wide. The width has been reduced to 0.25 [m] and the usable length is 7 [m]. A sketch of the experimental facility used for systematic tests is shown on Figure 1. The state of the flume during and after the experiment can be seen on Figure 2.

Two sets of experiments are used in this paper to show the impact of boulder distance and diameter on the sediment transport capacity.

In both sets of experiments, a camcorder (25fps) is placed on the top of the central part of the flume. Peak flow velocities v [m/s] are measured with an ink tracer and video analysis. Flow discharge is measured with an electromagnetic flow-meter, this value is then transformed in a water discharge per unit width (0.25 [m]) q [m^2/s]. Boulder protrusion and channel morphology is measured at the end of the experiment with a laser. The main differences are the sediment supply and bedload measurement, which is represented by the sediment discharge per unit width (0.25 [m]) q_s [m^2/s].

Preliminary experiments (Table 2) were carried out on a less complex experimental facility (Ghilardi et al., 2011). Flume slope was 6.7% and only boulders of average diameter of 0.075 [m] have been used for this set of experiments. Values of dimensionless boulders distances λ/D between 2.4 and 4.2 were used. For these preliminary experiments, the sediment supply occurred manually and the sediment outlet was measured only punctually at the end of the experiment. Sediment supply was adjusted to reach equilibrium conditions for a given water discharge. Sediments were not directly recirculated. This preliminary set of experiments is used to show the effect of boulder distance on sediment transport.

Systematic tests (Table 3) are now carried out, on an improved facility. The sediment supply is done by a calibrated sediment feeder and the sediment outlet is measured almost continuously. Water discharge is changed during the experiment to reach equilibrium conditions for a given sediment supply. Sediments are recirculated. Boulders of mean diameter 0.075, 0.100 and 0.125 [m] are used. Values of λ/D equal 2, 3 and 5 are used. The flume slope is 6.6%. This second set of data is used to show the impact of boulder diameter and distance on the bedload transport capacity.

For both sets of experiments, an initial flat bed is prepared with mobile sediments (Table 1). This grain

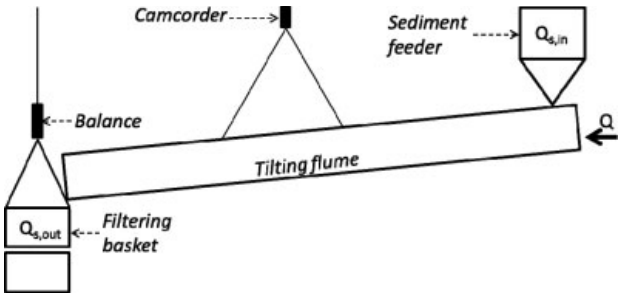

Figure 1. Sketch of the systematic experimental facility.

Figure 2. $\lambda/D = 3$, $D = 0.125$ [m], $q = 0.0235$ [m2/s], $q_s = 0.119*10^{-3}$ [m^2/s]. During the experiment on the left, and after the experiment on the right.

size distribution also corresponds to that of the mobile part of the bed. Natural boulders of diameter D are then placed randomly in the flume with a certain distance λ, in order to obtain chosen values of λ/D. The position of boulders for a given couple D and λ/D is the same in all the experiments of a given set of data (preliminary or systematic).

The immobile bed proportion A_i/A_t [−], where A_i [m^2] is the bed area occupied by boulders and A_t [m^2] the total bed area, is calculated based on top pictures of the flume. P [%] is the boulder protrusion with respect to the diameter of the equivalent sphere of diameter D. This value is calculated based on the measured absolute average protrusion P_{av} [m]. The discharge ratio q_s/q [−] is also useful to compare tests.

Table 1. Grain size distribution of the supplied sediments.

d_{30} [mm]	d_{50} [mm]	d_m [mm]	d_{90} [mm]
5.1	6.9	9.1	14.2

3 EXPERIMENTAL RESULTS

3.1 *Protrusion and hydraulic jumps*

As observed on steps in mountain streams, the upstream protrusion of the boulders is smaller than the downstream protrusion. The correlation between these values is however extremely high ($R^2 = 0.95$). During the experiments it is observed that the downstream protrusion is 1.5 times the upstream protrusion (Figure 3). The average protrusion is also tightly linked with the upstream and the downstream protrusion. For means of comparison between experiments it is thus

Table 2. Table of preliminary experiments parameters and results. All the experiments are carried out on a flume with a slope of 6.7% and 0.25 [m] wide.

Test No.	λ/D [−]	D [m]	q_s [m^2/s] $*10^{-3}$	q [m^2/s]	v [m/s]	P_{av} [m]	P [%]	A_i/A_t [−] $*10^{-2}$	q_s/q [−] $*10^{-3}$
1	0	0.075	0.362	0.0200	0.80	0.000	0.0	0.0	18.10
2	0	0.075	0.305	0.0200	0.82	0.000	0.0	0.0	15.20
3	0	0.075	0.534	0.0300	1.12	0.000	0.0	0.0	17.80
4	4.2	0.075	0.272	0.0200	0.94	0.022	29.5	3.9	13.60
5	4.2	0.075	0.468	0.0300	0.91	0.025	32.9	3.8	15.60
6	4.2	0.075	0.402	0.0300	0.91	0.027	35.3	3.9	13.40
7	3.0	0.075	0.204	0.0200	0.79	0.018	24.4	6.6	10.20
8	3.0	0.075	0.361	0.0300	0.98	0.026	34.7	7.1	12.00
9	3.0	0.075	0.350	0.0300	0.98	0.028	37.1	7.6	11.70
10	3.0	0.075	0.542	0.0400	1.12	0.032	42.0	7.0	13.50
11	2.4	0.075	0.131	0.0200	0.79	0.022	28.8	13.0	6.60
12	2.4	0.075	0.276	0.0300	0.91	0.028	37.3	13.3	9.20
13	2.4	0.075	0.400	0.0400	1.02	0.027	35.9	13.3	10.00

Table 3. Table of systematic experiments parameters and results. All the experiments are carried out on a flume with a slope of 6.6% and 0.25 [m] wide.

Test No.	λ/D [−]	D [m]	q_s [m^2/s] $*10^{-3}$	q [m^2/s]	v [m/s]	P_{av} [m]	P [%]	A_i/A_t [−] $*10^{-2}$	q_s/q [−] $*10^{-3}$
1	0	0.000	0.151	0.0204	0.80	0.000	0.0	0.0	7.40
2	0	0.000	0.115	0.0162	0.74	0.000	0.0	0.0	7.06
3	3	0.125	0.171	0.0240	0.93	0.032	25.4	8.4	7.11
4	3	0.100	0.155	0.0240	0.84	0.025	25.0	9.3	6.48
5	2	0.100	0.059	0.0228	0.86	0.021	21.0	21.7	2.58
6	3	0.075	0.097	0.0212	0.86	0.022	29.0	10.7	4.56
7	2	0.125	0.080	0.0228	0.83	0.024	19.0	19.1	3.51
8	2	0.075	0.027	0.0209	0.80	0.019	25.0	18.4	1.30
9	3	0.125	0.116	0.0236	0.84	0.048	38.6	9.0	4.92
10	5	0.100	0.136	0.0223	0.91	0.047	47.2	3.4	6.09
11	5	0.075	0.128	0.0222	0.87	0.034	45.7	3.2	5.79
12	5	0.125	0.140	0.0208	0.98	0.056	44.9	3.0	6.76
13	3	0.075	0.142	0.0238	0.98	0.029	38.7	9.5	5.97
14	3	0.125	0.119	0.0235	0.92	0.043	34.3	8.9	5.08
15	3	0.100	0.124	0.0233	0.87	0.035	35.0	9.4	5.31

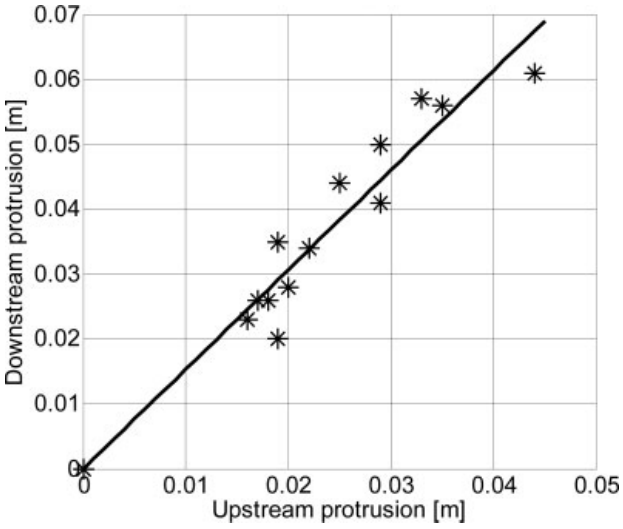

Figure 3. Correlation between upstream (P_{us}) and downstream (P_{ds}) boulder protrusion. The trend line equation is $P_{ds} = 1.53*P_{us}$, with an R^2 of 0.95. Systematic data set (Table 3).

not relevant which protrusion to use. It will become relevant when used in a sediment transport equation, as suggested by Yager et al. (2007). Yager et al. (2007) used a percentage value of the protrusion for comparison between test results. This doesn't seem adequate anymore when different boulder sizes are used during the experiments.

In the present paper percentage boulder protrusion P are calculated with respect to the theoretical equivalent sphere diameter D, and not with respect to each real boulder form. This will induce a difference in percentage protrusion of 12–15%, because the boulders are always oriented with the long axis in the flow direction and the short axis perpendicular to the bed, as suggested by Canovaro et al. (2007).

Figure 4 shows the flow conditions during experiments with similar bedload, for the reference test and for varying boulder diameters for a $\lambda/D = 5.0$.

The flow surface becomes more turbulent when boulders are presents, dissipating energy that will not be used to mobilize sediments any more.

During experiments without boulders, no hydraulic jumps can normally be seen. On the other hand, hydraulic jumps are clearly visible in experiments with macro-roughness elements, if the protrusion of the boulders is big enough. Hydraulic jumps have an important local impact, causing the scouring downstream of boulders. The bigger is the protrusion and the higher the number of hydraulic jumps.

In Figure 4, with $\lambda/D = 5$, it appears that the flow surface is more constant for larger boulders diameters. For these experiments the sediment transport was increasing with the boulder diameter.

3.2 *Sediment pulses*

Systematic experiments, with a continuous bedload measurement, have shown huge fluctuations in sediment discharge in time. In the present research, both

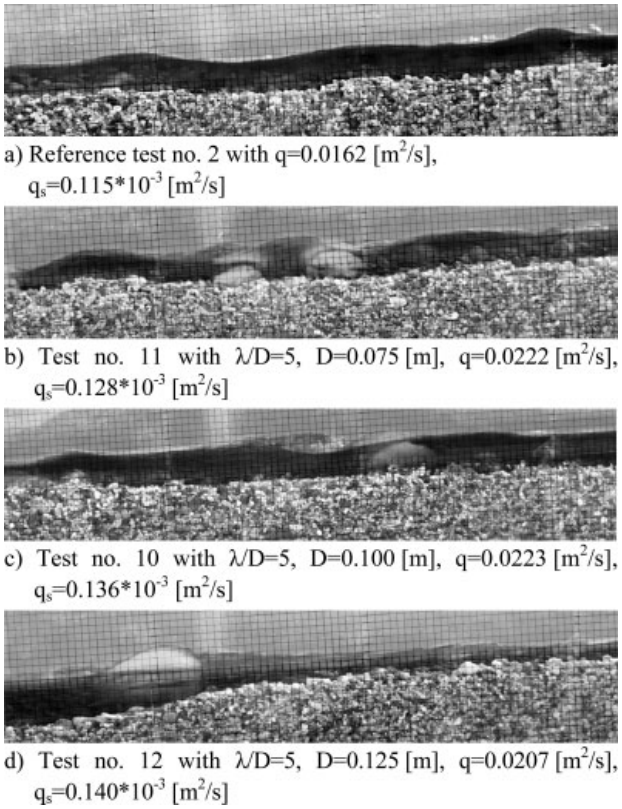

a) Reference test no. 2 with q=0.0162 [m^2/s], q_s=0.115*10^{-3} [m^2/s]

b) Test no. 11 with λ/D=5, D=0.075 [m], q=0.0222 [m^2/s], q_s=0.128*10^{-3} [m^2/s]

c) Test no. 10 with λ/D=5, D=0.100 [m], q=0.0223 [m^2/s], q_s=0.136*10^{-3} [m^2/s]

d) Test no. 12 with λ/D=5, D=0.125 [m], q=0.0207 [m^2/s], q_s=0.140*10^{-3} [m^2/s]

Figure 4. Flow conditions during the reference experiment and varying boulder diameters for a similar bedload transport and $\lambda/D = 5$. Systematic data set (Table 3).

of the phenomena mentioned by Iseya et al. (1987) and Frey et al. (2003), namely bedforms migration and grain sorting, have been visually observed. The migration of bedforms seems to be dominant in reference tests, without boulders. Gravel bars and riffles regularly forms and rapidly get destroyed during the experiment. The grain size distribution (GSD) on riffles is visually coarser than the average surface GSD. Deposition creates an almost horizontal bed followed by a steep part with rapid flow (Figure 5). When the flow becomes too fast, some grains are eroded downstream of the riffle. The whole structure is then rapidly destroyed and sediment discharge increases drastically. The cycle of riffles formation and destruction continues during all the experiment.

During experiments with boulders some rapid changes in bed morphology and especially erosion and deposition around boulders has been observed (Figure 6).

Segregation of surface GSD has also been visually identified. During low sediment transport event mainly coarse grains are leaving the flume and the surface GSD becomes coarser.

These sediment pulses may explain the generally higher sediment discharge measured during preliminary tests. It is possible that the punctual measurements done over 5 minutes took place during high sediment fluxes (Figure 7). Moreover, the flume slope for preliminary tests is slightly higher and the protrusion of boulders is generally lower than for systematic tests (Table 2 and Table 3). As shown by Yager et al.

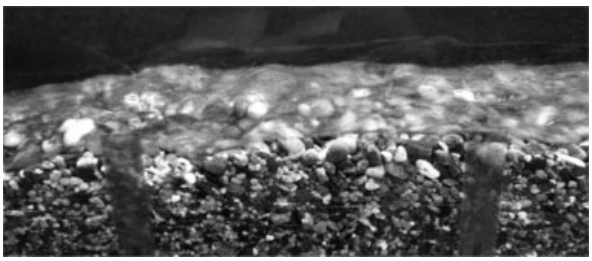

Figure 5. Coarse riffle formation in reference tests without boulders. Test no. 2 of the systematic data set (Table 3).

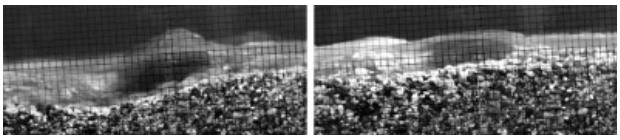

Figure 6. Rapid variation in boulder protrusion. On the left the boulder at time 0 and on the right the same boulder 5 minutes later. Test no. 11 with $\lambda/D = 5$, $D = 0.075$ [m], $q = 0.0207$ [m^2/s], $q_s = 0.140*10^{-3}$ [m^2/s]. Systematic data set (Table 3).

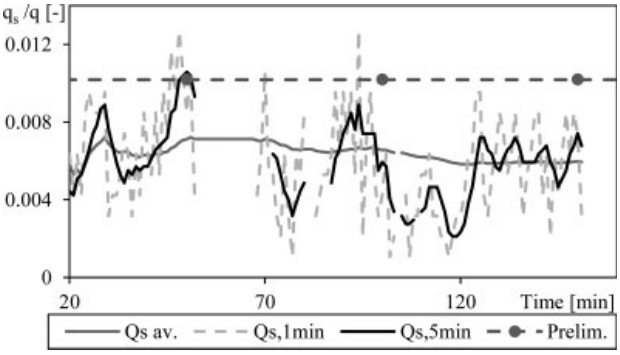

Figure 7. Discharge ratio q_s/q in time for the systematic experiments no. 13 with $\lambda/D=3$, $D = 0.075$ [m], $q = 0.0238$ [m^2/s], $q_s = 0.142*10^{-3}$ [m^2/s]. 'Qs,av' represents the average on the whole experiment time, 'Qs,1min' is the flux over 1 minute, 'Qs,5min' over 5 minutes. Some discontinuities are present because of the filtering basket emptying. "Prelim." represents the point value measured for the preliminary experiment no. 7 with $\lambda/D = 3$, $D = 0.075$ [m], $q = 0.02$ [m^2/s] and $q_s = 0.204*10^{-3}$ [m^2/s]

(2007) a boulder with smaller protrusion would have less impact on the sediment transport.

3.3 *Influence of boulder distance*

Preliminary experiments (Table 2) have been carried out in order to analyze the impact of the dimensionless boulder distance on the sediment transport. All tests were performed with boulders of average diameters of 0.075 [m]. Tests no. 1 to no. 3 are reference tests without boulders. A more detailed table of experiments is presented in Ghilardi et al. (2011). During these experiments the sediment outlet was measured punctually at the end of the experiment.

Preliminary tests have shown that an increase in boulder spatial density (decreasing λ/D) causes a decrease in sediment transport capacity (Figure 8).

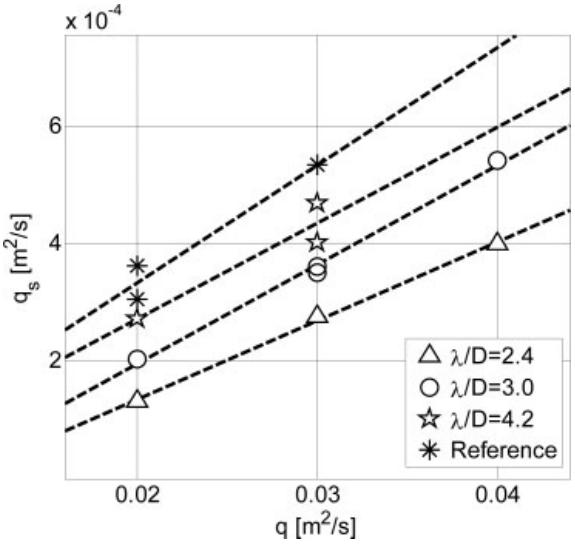

Figure 8. Sediment discharge q_s as a function of water discharge q for varying boulder spacing, for a diameter of 0.075 [m]. Preliminary data set (Table 2) is grouped by λ/D, with their trendlines.

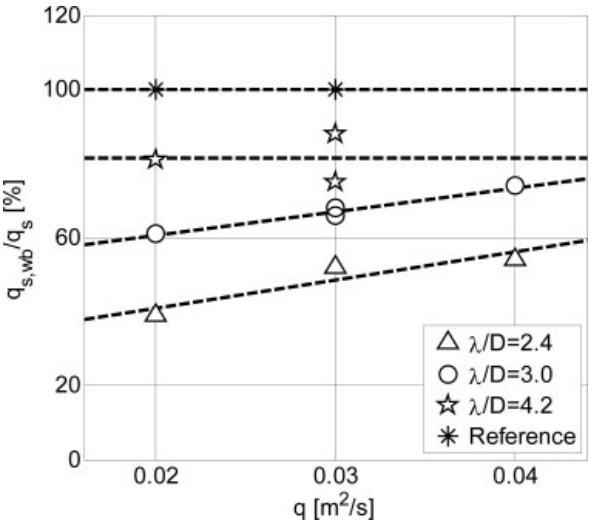

Figure 9. Sediment discharge ratio between experiments without boulders $q_{s,wb}$ and with boulders q_s for varying λ/D spacing and discharges q, for a diameter of 0.075 [m]. Preliminary data set (Table 2) is grouped by λ/D, with their trendlines.

The impact of the boulders on sediment transport capacity is decreased by an increase in water discharge (Figure 9). This is due to the decreased relative roughness created by the boulder. For a small distance between boulders ($\lambda/D = 2.4$) the sediment outlet is only 42% of the transport without boulders for the same discharge of 0.02 [m^2/s]. When the discharge increases to 0.04 [m^2/s], the macro-roughness elements decrease the sediment discharge to 57% of the reference capacity.

Figure 10 shows that the discharge ratio q_s/q decreases as a function of the immobile bed proportion multiplied by the average protrusion. Data are clearly grouped by boulder distances. In fact, both of these parameters, namely immobile surface and protrusion,

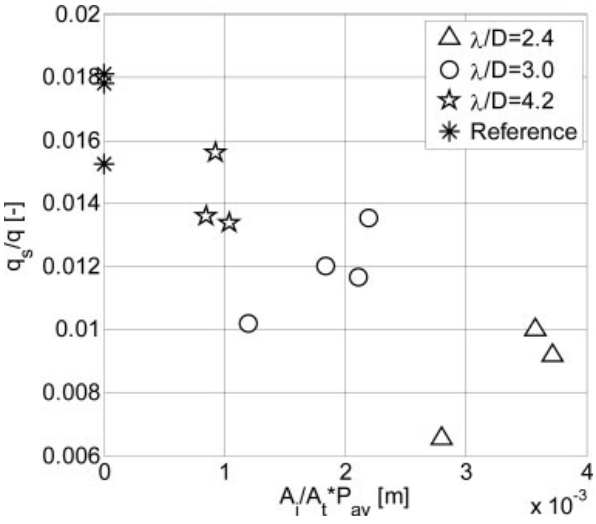

Figure 10. Discharge ratio q_s/q as a function of the immobile bed proportion A_i/A_t multiplied by the average P_{av}. Preliminary data set (Table 2) is grouped by λ/D, with their trendlines.

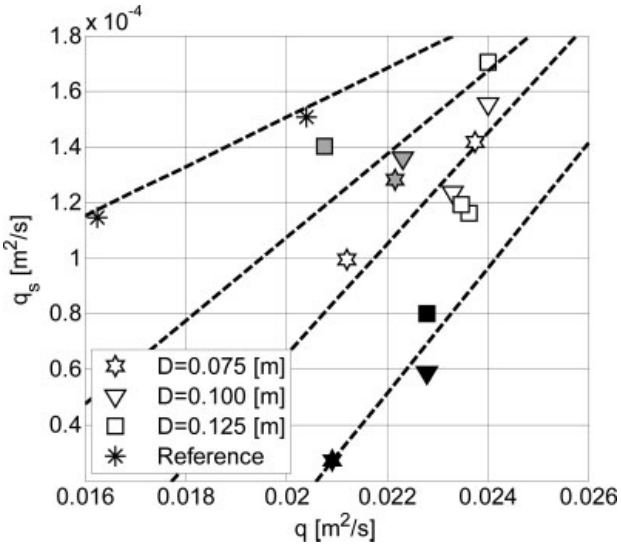

Figure 11. Sediment discharge q_s as a function of water discharge q for varying boulder diameters, indicated by the form of the point. Colors represent the boulder dimensionless spacing. Black points represents λ/D = 2, white points λ/D = 3 and gray points λ/D = 5. Trendlines indicate trends for each λ/D value. Systematic data set (Table 3).

have an impact on sediment transport. Discharge ratio decreases with a decreasing λ/D.

Ghilardi et al. (2011) showed that considering the presence of immobile boulders as suggested by Yager et al. (2007) clearly improves the performance of many sediment transport formulae. This is because the bed area occupied by immobile boulders and their protrusion should be taken into account. The presence of boulders reduces the shear stress available for sediment transport.

3.4 *Influence of boulder diameter*

Systematic tests are carried out on an improved experimental facility in order to determine the impact of the boulder diameter and position on sediment transport capacity. The list of experiments is presented in Table 3. Tests no. 1 and no. 2, with λ/D = 0 are reference tests, carried out without boulders. Tests no. 2 and no. 10 to no. 15 have similar sediment transport.

It can be noticed than even for experiments with varying boulder diameters the sediment transport decreases with a decreasing λ/D (Figure 11). The difference in sediment transport between λ/D = 3 and λ/D = 5 is smaller than between λ/D = 2 and 3. This confirms Yager et al. (2007) theory, stating that the impact of boulders decreases rapidly as λ/D increases. The direct influence of the boulder diameter is less clear. It seems however that the sediment transport increases with an increasing diameter. This is probably related to the absolute number of boulders, and thus of hydraulic jumps, present. The dissipation of energy for one boulder is higher if the diameter and the protrusion are bigger, but the total number of boulders is smaller for a given λ/D if the boulder diameter is bigger.

The average protrusion P_{av} of the boulders seems to increase with q_s/q and with λ/D. Although no direct link can be identified between λ/D and the protrusion

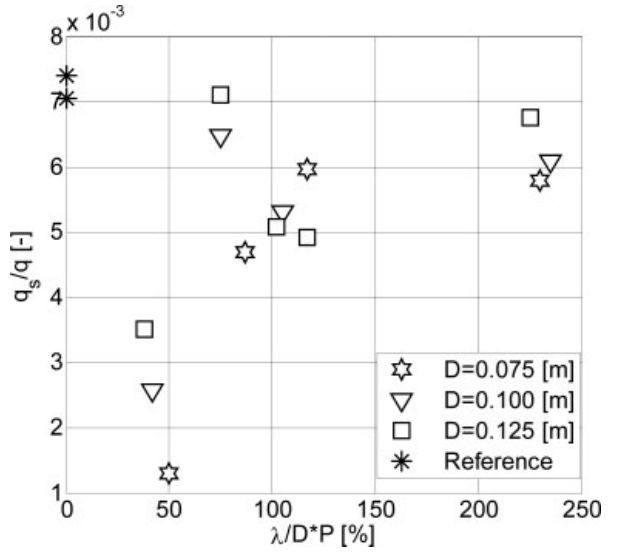

Figure 12. Discharge ratio q_s/q as a function of boulder protrusion P and dimensionless distance λ/D. Systematic data set (Table 3) is grouped by diameter.

P of boulders as a function of their diameter, a relationship between the discharge ratio q_s/q and λ/D*P is visible (Figure 12). These trends can also be shown as a function of the immobile bed proportion A_i/A_t, multiplied by their average protrusion P_{av}. These two parameters represent the loss of surface contributing to sediment transport (A_i/A_t) and the loss of energy due to the boulders (P_{av}). As Figure 13 shows, the discharge ratio increases with the surface occupation and protrusion increase, for a given λ/D, for varying boulders diameters. This confirms the trend already seen in preliminary tests for an average boulder diameter of 0.075 [m]. When looking at the diameter influence alone, the tendency is less clear. However the trend

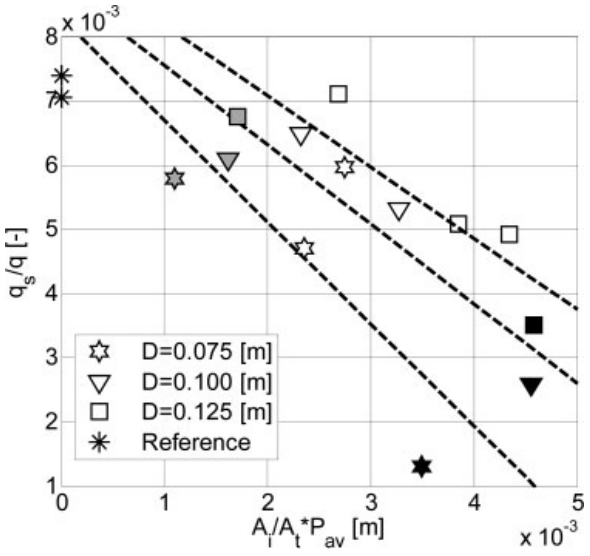

Figure 13. Discharge ratio q_s/q as a function of the proportion of the bed total area A_t occupied by the immobile boulders A_i multiplied by the average P_{av}. Points form indicates the diameter. Their color indicates the distance. Black points represents $\lambda/D = 2$, white points $\lambda/D = 3$ and gray points $\lambda/D = 5$. Trendlines indicate trends for each D value. Systematic data set (Table 3).

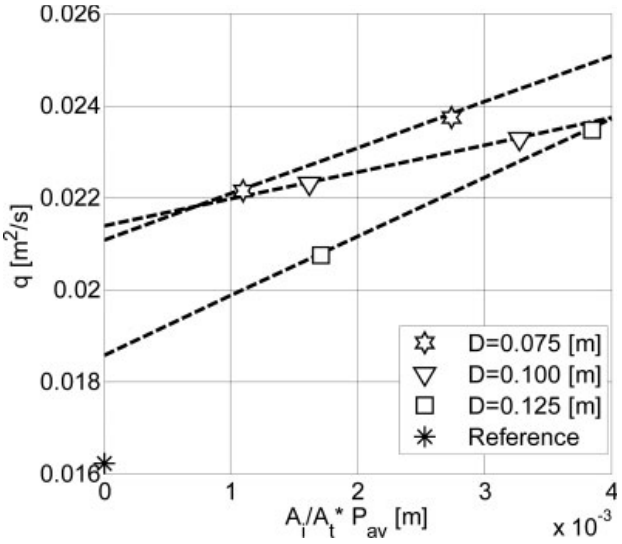

Figure 14. Water q discharge as a function of the proportion of the bed total area A_t occupied by the immobile boulders A_i multiplied by the average P_{av}. For tests no. 2 and no. 10 to no. 15, which have similar sediment discharges. Systematic data set (Table 3) is grouped by diameter, with their trendlines.

lines indicate that for a given discharge ratio the surface occupation times the average protrusion tends to increase with the diameter.

Figure 14, using only tests no. 2 and no. 10 to no. 15 for similar sediment discharge, seem to indicate that for a given immobile bed proportion multiplied by the average protrusion, the equilibrium water discharge decreases as the boulder diameter increases. This is possibly due to the fact that the number of hydraulic jumps is bigger for a smaller boulder diameter for a given λ/D. Figure 15 indicates that the sediment

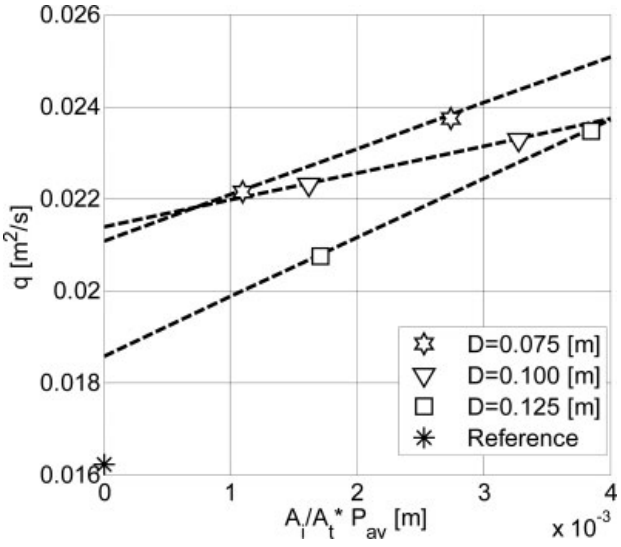

Figure 15. Water discharge as a function of the boulder diameter. For tests no. 2 and no. 10 to no. 15, which have similar sediment discharges. Systematic data set (Table 3) is grouped by λ/D, with their trendlines.

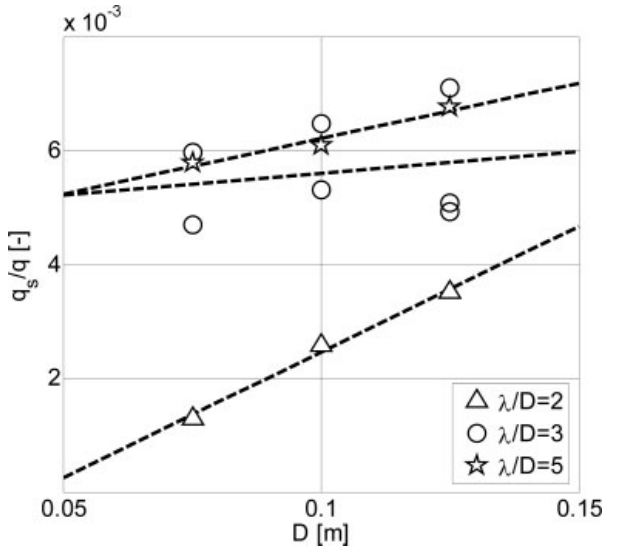

Figure 16. Discharge ratio q_s/q as a function of the diameter D. Systematic data set (Table 3) is grouped by λ/D, with their trendlines.

transport reduction is not directly linked only to the boulder diameter. Even if the equilibrium water discharge for an almost constant sediment transport is higher for $D = 0.075$ [m] than for $D = 0.125$ [m] for both the dimensionless boulder distances λ/D.

This trend is confirmed by Figure 16, where it can be noticed that the discharge ratio tend to increase with the boulder diameter, for all dimensionless boulder distances λ/D, although the trend is not clear for $\lambda/D = 3$.

The impact of boulders on peak flow velocities is not so clear, though it seems that the velocity increases with an increase in boulder distances and diameter (Figure 17). Further analysis taking into account average flow velocities need to be carried out.

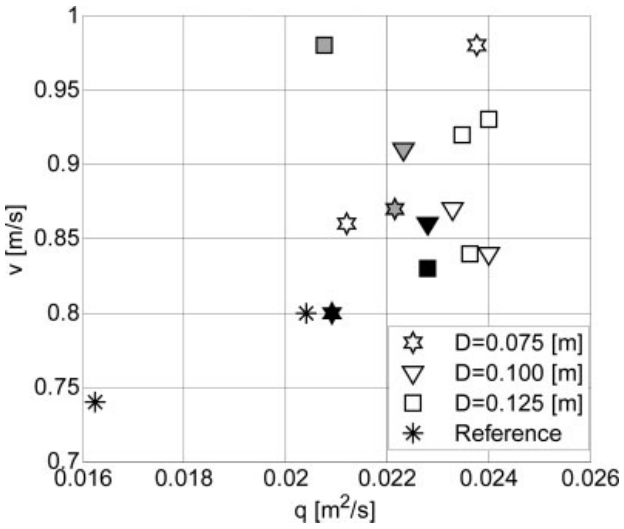

Figure 17. Peak flow velocity v as a function of water discharge. Points form indicates the diameter. Their color indicates the distance. Black points represents $\lambda/D = 2$, white points $\lambda/D = 3$ and gray points $\lambda/D = 5$. Systematic data set (Table 3).

4 CONCLUSIONS

The present study has clearly shown that the presence of macro-roughness elements, such as large immobile boulders, decrease the sediment transport capacity of a steep river. The smaller the boulder spacing, the smaller the sediment discharges. The impact of the boulder diameter is less clear, but it seems that a bigger diameter has less influence on sediment transport, for a given dimensionless spacing. This is probably due to the smaller number of boulders needed, and thus the smaller number of hydraulic jumps dissipating energy.

Sediment pulses have been observed due to the wide grain size distribution used.

Further experiments will be carried out, including also different flume slopes.

AKNOWLEDGMENTS

The present study has been financed by the Swiss Competence Center for Environmental Sustainability (CCES) of the ETH domain and the Swiss Federal Office of Energy (SFOE)

REFERENCES

Bacchi, V., Recking, A., Frey, P., Naaim, M. 2009. Experimental measurement of bedload and slope fluctuations in a channel under constant feed and water conditions, Proc. of 33th IAHR world congress, Vancouver, 1–14 August 2009.

Bathurst, J.C. 1978. Flow resistance of large-scale roughness. *Journal of hydraulics division. Proceedings of the American Society of Civil Engineers* 104 (HY12): 1587–1603.

Canovaro, F., Paris, E., Solari, L. 2007. Effects of macroscale bed roughness geometry on flow resistance. *Water Resources Research* 43 W10414, doi:10.1029/2006 WR005727.

Ferro, V. 1999. Friction factor for gravel-bed channels with high boulder concentration. *Journal of Hydraulic Engineering* 125 (7): 771–778.

Frey, P., Ducottet, C., Jay, J. 2003. Fluctuations of bed load solid discharge and grain size distribution on steep slopes with image analysis. *Experiments in fluids* 35: 589–597.

Ghilardi, T., Schleiss, A. J. 2001. Influence of immobile boulders on bedload transport in a steep flume. *Proc. of 34th IAHR World Congress, Brisbane, 26 June–1st July 2011.*

Iseya, F., Ikeda, H. 1987. Pulsations in bedload transport rates induced by a longitudinal sediment sorting: A flume study using sand and gravel mixtures. *Geografiska Annaler (A)* 69: 15–27.

Lenzi, M.A., D'Agostino, V., Billi, P. 1999. Bedload transport in the instrumented catchment of the Rio Cordon – Part I: Analysis of bedload records, conditions and threshold of bedload entrainment. *Catena* 36: 171–190.

Lenzi M.A., Mao L., Comiti F. 2006. When does bedload transport begin in steep boulder-bed streams? *Hydrol. Process.* 20: 3517–3533.

Papanicolaou, A.N., Bdour, A., Wicklein, E. 2004. One-dimensional hydrodynamic/sediment transport model applicable to steep mountain streams. *Journal of Hydraulic Research* 42 (4): 357–375.

Recking, A. 2006. Etude expérimentale de l'influence du tri granulométrique sur le transport solide par charriage. Thesis dissertation. N° d'ordre : 2006-ISAL-00113. Institut National des Sciences appliquées de Lyon.

Rickenmann, D. 2001. Comparison of bed load transport in torrents and gravel bed streams. *Water Resources Research* 37 (12): 3295–3305.

Yager, E.M., Kirchner, J.W., Dietrich, W.E. 2007- Calculating bed load transport in steep boulder bed channels. *Water Resources Research* 43, W07418, doi:10.1029/2006 WR005432.